ENVIRONMENTAL RESEARCH
LETTERS

PURPOSE-LED PUBLISHING™
Celebrating the 20th anniversary of Environmental Research Letters

LETTER • **OPEN ACCESS**

Does higher-resolution climate forcing improve impact model performance?

To cite this article: Johanna T Malle *et al* 2026 *Environ. Res. Lett.* **21** 204028

View the article online for updates and enhancements.

You may also like

- Fast climate impact emulation for global temperature scenarios with the rapid impact model emulator (RIME)
Edward Byers, Michaela Werning, Mahé Perrette et al.
- Implications of regional improvement in global climate models for agricultural impact research
Julian Ramirez-Villegas, Andrew J Challinor, Philip K Thornton et al.
- Uncertainty constraints on economic impact assessments of climate change simulated by an impact emulator
Hideo Shiogama, Jun'ya Takakura and Kiyoshi Takahashi

This content was downloaded from IP address 91.227.109.26 on 27/10/2026 at 11:31

ENVIRONMENTAL RESEARCH
LETTERS

Check for updates

OPEN ACCESS

RECEIVED
29 April 2026

REVISED
25 September 2026

ACCEPTED FOR PUBLICATION
9 October 2026

PUBLISHED
27 October 2026

Original content from this work may be used under the terms of the Creative Commons Attribution 4.0 licence.

Any further distribution of this work must maintain attribution to the author(s) and the title of the work, journal citation and DOI.

LETTER

Does higher-resolution climate forcing improve impact model performance?

Johanna T Malle[1,2,*], Christopher P O Reyer[3], Yael Amitai[4], Andrey L D Augustynczik[5], Yaron Be'eri-Shlevin[4], Elad Ben-Zur[7], Peter Burek[6], Tarunsinh Chaudhari[8], Jinfeng Chang[9,30], Alessio Collalti[10], Daniela Dalmonech[10], Shouro Dasgupta[11,12], Iulii Didovets[3], Marc Djahangard[13], Laura Dobor[14], Louis François[8], Simon N Gosling[15], Fred F Hattermann[3], Shaochun Huang[16], Heike Lischke[2], Thomas Lorimer[17,27,28], Katarína Merganičová[14,19], Francesco Minunno[18,20], Mats Nieberg[3,21,22], Elizabeth J Z Robinson[12], Martin Schmid[17], Mikhail Smilovic[6,29], Ritika Srinet[18,20], Elia Vangi[10], Xue Yang[23], Rasoul Yousefpour[13,24], Ana I Ayala[26], Daniel Mercado-Bettin[25], Dánnell Quesada-Chacón[3] and Dirk N Karger[2]

[1] Department of Evolutionary Biology and Environmental Studies, University of Zurich, Zurich, Switzerland
[2] Dynamic Macroecology, Land Change Science, Swiss Federal Institute for Forest, Snow and Landscape Research WSL, Birmensdorf, Switzerland
[3] Potsdam Institute for Climate Impact Research (PIK), Member of the Leibniz Association, Potsdam, Germany
[4] Kinneret Limnological Institute, Israel Oceanographic & Limnological Research, Migdal, Israel
[5] Integrated Biosphere Futures Research Group, Biodiversity and Natural Resources Program, International Institute for Applied Systems Analysis (IIASA), Laxenburg, Austria
[6] Water Security Research Group, Biodiversity and Natural Resources Program, International Institute for Applied Systems Analysis (IIASA), Laxenburg, Austria
[7] Institute of Earth Sciences, Hebrew University of Jerusalem, Jerusalem, Israel
[8] Department of Astrophysics, Geophysics and Oceanography (AGO), SPHERES Research Unit, University of Liège, Liège, Belgium
[9] State Key Laboratory of Soil Pollution Control and Safety, College of Environmental and Resource Sciences, Zhejiang University, Hangzhou 310058, People's Republic of China
[10] Forest Modelling Lab., Institute for Agriculture and Forestry Systems in the Mediterranean, National Research Council of Italy (CNR-ISAFOM), Perugia 06128, Italy
[11] Centro Euro-Mediterraneo sui Cambiamenti Climatici (CMCC), Venice, Italy
[12] Grantham Research Institute on Climate Change and the Environment, London School of Economics and Political Science (LSE), London, United Kingdom
[13] Chair of Forestry Economics and Forest Planning, University of Freiburg, Freiburg, Germany
[14] Faculty of Forestry and Wood Sciences, Czech University of Life Sciences, Prague, Czech Republic
[15] School of Geography, University of Nottingham, Nottingham, United Kingdom
[16] The Norwegian Water Resources and Energy Directorate (NVE), Oslo, Norway
[17] Surface Waters—Research and Management, Eawag: Swiss Federal Institute of Aquatic Science and Technology, Kastanienbaum, Switzerland
[18] Institute for Atmospheric and Earth System Research (INAR) & Faculty of Agriculture and Forestry, University of Helsinki, Helsinki, Finland
[19] Department of Biodiversity of Ecosystems and Landscape, Institute of Landscape Ecology, Slovak Academy of Sciences, Bratislava, Slovakia
[20] Forest Modelling, Yucatrote, Lagos, Portugal
[21] European Forest Institute, Bonn, Germany
[22] Chair of Forest Growth and Woody Biomass Production, TU Dresden, Tharandt, Germany
[23] State Key Laboratory of Water Engineering Ecology and Environment in Arid Area, Xi'an University of Technology, Xi'an, People's Republic of China
[24] John H. Daniels Faculty of Architecture, Landscape, and Design, University of Toronto, Toronto, Canada
[25] Spanish National Research Council, Centre for Advanced Studies Blanes, Blanes, Spain
[26] Limnology Unit, Department of Ecology and Genetics, Uppsala University, Uppsala, Sweden
[27] Laboratory of Molecular and Behavioral Neuroscience, Institute for Neuroscience, Department of Health Sciences and Technology, ETH Zurich, Switzerland
[28] ETH Zurich 3R Hub, ETH Zurich, Switzerland
[29] Institute of Environmental Engineering, ETH Zurich, 8093 Zürich, Switzerland
[30] International Institute for Applied Systems Analysis (IIASA), Laxenburg, Austria
[*] Author to whom any correspondence should be addressed.

E-mail: johanna.malle@uzh.ch

Keywords: ISIMIP, high-resolution climate data, climate change impact modelling, CHELSA

Supplementary material for this article is available online

© 2026 The Author(s). Published by IOP Publishing Ltd

Abstract

Climate-impact assessments increasingly use high-resolution climate forcing, often assuming that finer spatial detail improves impact projections. Yet this assumption has rarely been tested systematically across impact sectors, regions, and forcing variables. Here we use coordinated simulations from 16 impact models participating in the Inter-Sectoral Impact Model Intercomparison Project to evaluate how increasing forcing resolution from 60 km to 10 km, 3 km, and 1 km affects both climate-input accuracy and impact-model performance. We find that most gains occur when moving from 60 km to 10 km resolution. Further refinement to 3 km and 1 km yields smaller and less consistent benefits, and in some cases degrades performance. Improvements are strongest for temperature-sensitive models and in topographically complex regions, where finer forcing better captures spatial gradients. By contrast, precipitation-driven models and low-relief regions show weaker and less systematic gains. These results challenge the expectation that ever-finer climate forcing necessarily improves impact modelling. Instead, the value of resolution depends on the forcing variable, sector, region, and process representation of the impact model. Benchmarking resolution choices against impact-model performance, rather than climate-input accuracy alone, is therefore essential for designing efficient and decision-relevant climate-impact assessments.

1. Introduction

Climate change is progressing rapidly and poses serious risks to both natural ecosystems and human societies (Chen *et al* 2021, Lee *et al* 2023). To assess these risks, climate impact models are widely applied across multiple sectors, including agriculture (Jägermeyr *et al* 2021), forestry (Reyer *et al* 2014, Lawrence *et al* 2022), terrestrial biodiversity (Cramer *et al* 2001, Habibullah *et al* 2022), hydrology (Goderniaux *et al* 2011, Woolway *et al* 2021, Wang *et al* 2025), energy (Isaac and van Vuuren 2009, Zapata *et al* 2022), water quality (Jones *et al* 2025), labor (Dasgupta *et al* 2021) and human health (Caminade *et al* 2014, Smith *et al* 2024). These models are inherently complex, integrating a wide range of biophysical and socioeconomic processes. As a result, they carry substantial uncertainty, which is further amplified when driven by inherently complex future climate scenarios.

To address and disentangle these uncertainties and enhance the comparability of results, international initiatives such as the Inter-Sectoral Impact Model Intercomparison Project (ISIMIP) (Frieler *et al* 2017) provide harmonized protocols and standardized input datasets to facilitate inter-model and cross-sectoral comparisons. This approach is inspired by practices from the climate modeling community, where coordinated model intercomparison projects like CMIP (Meehl *et al* 2000, 2007) have long used ensembles of simulations to assess uncertainty and model performance (Eyring *et al* 2016). However, truly interdisciplinary climate impact assessments that integrate models from multiple sectors under common forcing conditions are still in their infancy (Harrison *et al* 2016, Schipper *et al* 2021, Frieler *et al* 2024), despite increasing evidence that climate impacts are interconnected and often occur simultaneously across different ecosystems (Zscheischler *et al* 2018, Ciscar *et al* 2019, Ridder *et al* 2020, Pfenning-Butterworth *et al* 2024).

An important but often overlooked source of uncertainty in climate impact modeling stems from the discrepancy between the resolution of climate input data and the spatial scale at which impacts occur. Many impact models operate at coarse spatial resolutions (e.g. 0.5° or 50 km at the equator), which can mask fine-scale climatic variability, particularly in heterogeneous or mountainous terrain. This mismatch can significantly affect simulations of components of ecosystem dynamics such as water fluxes (Wada *et al* 2016), forest carbon fluxes (Harris *et al* 2021), growing seasons (McMaster and Wilhelm 1997), and species migration dynamics (Engler and Guisan 2009, Zani *et al* 2023). For example, climate data averaged over large grid cells may lead to inaccurate estimates of local temperature and precipitation, which are critical drivers of ecological processes.

Several sector-specific studies have already demonstrated that the spatial resolution of climate forcing data can substantially influence model outcomes, including for agriculture (Mearns *et al* 2001), biodiversity (Randin *et al* 2009, Seo *et al* 2009, König *et al* 2021), vegetation dynamics (Hickler *et al* 2012), hydrology (Hattermann *et al* 2017, Aerts *et al* 2022, Kumar *et al* 2022), including snow-specific processes (Magnusson *et al* 2019, Barnhart *et al* 2024), and climate variability (Karger *et al* 2023). However, a comprehensive, cross-sectoral analysis of spatial-scale effects using consistent climate input data has been lacking. A major barrier to such studies is the inconsistent application and, in some cases, limited availability of high-resolution climate forcing data across impact sectors and geographic regions. Models are often run only at one resolution or rely on regionally tuned downscaling approaches that vary in

methodology and coverage (Wood *et al* 2004, Keller *et al* 2022).

To address this gap, globally standardized, high-resolution climate datasets are needed. While coarse-resolution standardized data products are already available and widely used, for example within the ISIMIP framework (Lange 2019, Cucchi *et al* 2020), kilometer-scale standardized datasets are still scarce due to the computational challenges of running global climate models at such fine resolution (Dipankar *et al* 2015, Schär *et al* 2019). Current high-resolution simulations are limited by throughput constraints of even the most powerful supercomputers (Fuhrer *et al* 2018, Schulthess *et al* 2018, Neumann *et al* 2019, Bottazzi *et al* 2024). Available datasets and experimental setups are often restricted in spatial extent (Sun and Lan 2021, Baño-Medina *et al* 2022, Raffa *et al* 2023), limiting comprehensive analyses of spatial-scale effects.

Substantial research has addressed the challenge of reducing computational cost and runtime for downscaling. Less computationally demanding alternatives to dynamical downscaling include statistical downscaling and interpolation of observational and reanalysis data (Tabios and Salas 1985, Daly *et al* 1997, Thornton *et al* 1997, Reder *et al* 2025). However, observation-based interpolation methods often suffer from spatially uneven station densities (Briggs and Cogley 1996, Schneider *et al* 2014, Kidd *et al* 2017, Berndt *et al* 2018), which can distort model outputs. Downscaling reanalysis data using methods that correct for terrain and bias can offer a more consistent and scalable solution (Karger *et al* 2017, 2021).

In this study, we investigate how and to what extent the spatial resolution of climate forcing data affects the performance of climate impact models. Within the ISIMIP3a framework, we conducted standardized simulations using the CHELSA-W5E5 v1 climate data (Karger *et al* 2023) at four spatial resolutions (30″, 90″, 300″, and 1800″, corresponding to roughly 1, 3, 10, and 60 km) across 16 impact models from five different sectors (regional forest, regional water, lakes, biomes, and labor) with each model set up according to its sector-specific ISIMIP3a protocol (Frieler *et al* 2024). A map illustrating the geographic extent of impact model simulations across different regions and sectors is provided in figure 1. For each model and sector, we assess both the accuracy of the climate forcing data (precipitation and temperature) and the agreement between model outputs and observational data across the range of resolutions, with particular focus on how terrain complexity influences the results. This work contributes to the broader goal of enhancing transparency, comparability, and robustness in climate impact assessments, and aims to provide practical guidance on the scientific value of high-resolution forcing data.

2. Methods

2.1. Climate forcings and experiments

2.1.1. High-resolution forcing data: CHELSA-W5E5 v1.0

The CHELSA-W5E5 v1.0 dataset (Karger *et al* 2023), as included in the ISIMIP framework, provides global land-based climate data at a spatial resolution of 30″ (approximately 1 km at the equator) and daily temporal resolution, covering the period from 1979 to 2016. It includes the following variables: precipitation (pr), surface downwelling shortwave radiation (rsds), and daily mean, minimum, and maximum near-surface air temperature (tas, tasmin, tasmax). These data are derived through topographic downscaling of the W5E5 v1.0 observational dataset (original resolution 0.5°).

CHELSA-W5E5 v1.0 is produced using the CHELSA (Climatologies at High Resolution for the Earth's Land Surface Areas) v2.0 algorithm (Karger *et al* 2017, 2021, 2023). The downscaling process corrects for systematic biases associated with orographic features that are not adequately resolved in coarse-resolution data products.

The original 30″ data are spatially aggregated to coarser resolutions of 90″ (∼3 km, aggregation factor 3), 300″ (∼10 km, factor 10), and 1800″ (∼60 km, factor 60). Aggregation to 1800″ is necessary since the downscaled products differ from the default ISIMIP W5E5 data product at 0.5°/1800″. Because all coarser grids are derived from the same underlying 30″ fields rather than independently downscaled, climate inputs at adjacent resolutions are not fully independent, which may reduce apparent differences in model performance between resolutions.

All climate data are available at: https://data.isimip.org/search/query/chelsa/.

Because some impact models required additional variables at higher resolution, a scripting environment was provided (https://github.com/johanna-malle/w5e5_downscale) to downscale relative humidity, surface wind, air pressure, and longwave radiation, which are not yet supported by the CHELSA downscaling approach. The method for these variables is described in detail in Frieler *et al* (2024). For the high-resolution experiments, it was crucial to maintain consistent input forcings across resolutions wherever possible.

For further information on the climate forcing data used in the high-resolution sensitivity experiments, see Karger *et al* (2023) and Frieler *et al* (2024).

2.1.2. Experimental design

All four resolutions included in the CHELSA-W5E5 v1.0 dataset were included in the experimental design to evaluate whether higher-resolution atmospheric climate data enhance the performance of climate impact model simulations.

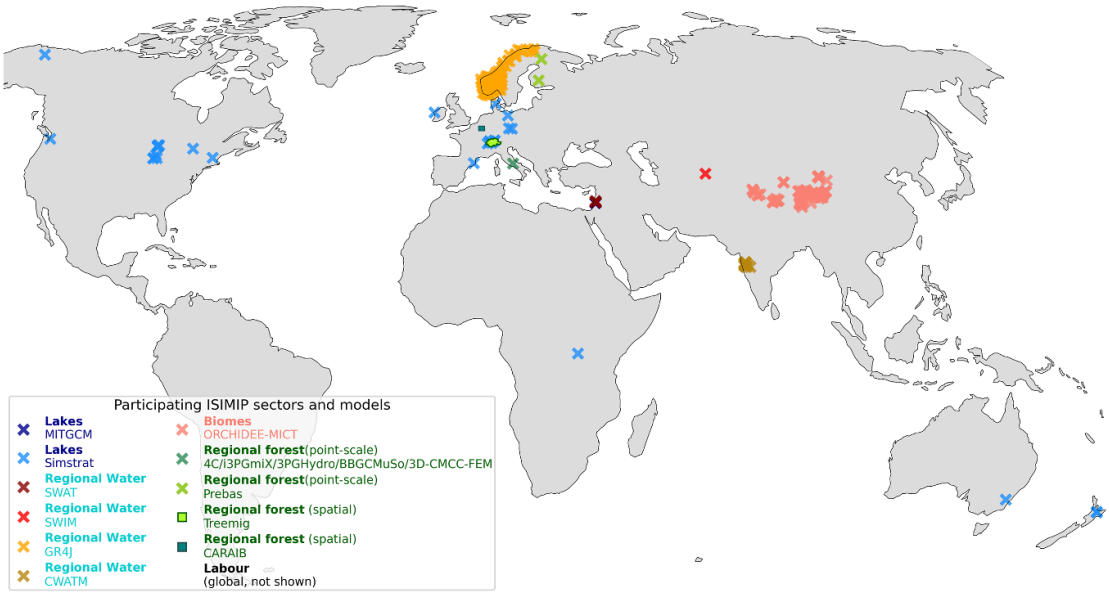


Figure 1. Overview of participating ISIMIP sectors and models, and location/geographic extent of the performed simulations.

These experiments aim to identify the resolution at which improvements in impact model simulations become evident when compared against observational impact indicators. Given the substantial storage and computational demands of daily 30″ data, this analysis is critical to determine the trade-offs between resolution and model performance.

Participating modeling groups were instructed to submit simulations for a minimum of two different spatial resolutions, along with corresponding observational data, to evaluate how the agreement between model output and observations varies with the spatial resolution of the climate forcing data and, for gridded models, with the resolution of the impact models themselves. The respective sector-specific ISIMIP3a simulation protocols were used as guidelines by all participating modeling groups. Depending on the sector and model, and constrained by the temporal resolution of the available observational data, simulated and observed variables were compared at daily, monthly, annual, or native model time-step resolution, as detailed in Supplementary Material A and B.

A more detailed description of the experimental design can also be found in Frieler *et al* (2024).

2.2. Participating sectors and impact models

The participating impact models in this study span a wide range of complexity, from relatively simple one-dimensional point-scale representations to sophisticated three-dimensional (3D) spatially explicit systems. These models differ in structural complexity, spatial scale, process representation, and sensitivity to climate-input resolution, both within and between sectors. Models simulated processes for different regions and at different resolutions (tables 1 and 2, figure 1). The geographic coverage was not selected as a statistically representative global sample, but instead reflects the spatial domains contributed by the participating ISIMIP models and the locations for which suitable observational data were available for model evaluation. Figure 1 should therefore be interpreted as the spatial coverage of this coordinated multi-model sensitivity experiment rather than as a globally representative sampling design.

Impact models from five different ISIMIP sectors were included in this analysis: Regional Forests, Regional Water, Lakes, Biomes, and Labor. Evaluation data include eddy-covariance flux tower measurements, river discharge records, reservoir level measurements, lake temperature profiles, and data on labor force outcomes from micro-surveys.

From the Regional Forests sector, five point-scale impact models participated (4C, i3PGmiX, 3PG-Hydro, Biome-BGCMuSo (BBGCMuSo), 3D-CMCC-FEM), all simulating at the same point location (Fluxnet site Collelongo, IT). One additional point-scale model (Prebas) was simulated at two locations in Finland, and two spatially distributed models (TreeMig, CARAIB) provided simulations across Switzerland and the area of Wallonia in Belgium/Netherlands, respectively. From the Regional Water sector, four models participated (CWatM, GR4J, SWAT, SWIM), each of which simulated different catchments. From the Lakes sector, two models participated (Simstrat and MITgcm), simulating 32 ISIMIP lakes and Lake Kinneret, respectively. These two lake models used different calibration strategies across the resolution experiments. Simstrat was recalibrated for each forcing resolution, whereas MITgcm used the same parameter set across all resolutions, initialized from a calibrated stable-state simulation. From the Biomes sector, one model

Table 1. Model overview (Part 1 of 2): sectors, spatial/model setup, region, temporal resolution, and number of evaluation sites.

Impact Model	Sector	Spatial Resolutions (arcsec)	Model Setup	Region	Temporal Resolution (internal/output)	No. of Eval. Sites
BBGCMuSo	Reg. Forest	30″, 90″, 300″, 1800″	point	Collelongo	daily/daily	1
3D-CMCC-FEM	Reg. Forest	30″, 90″, 300″, 1800″	point	Collelongo	daily/daily	1
i3PGmiX	Reg. Forest	30″, 90″, 300″, 1800″	point	Collelongo	monthly/monthly	1
4C	Reg. Forest	30″, 90″, 300″, 1800″	point	Collelongo	daily/daily	1
3PG-Hydro	Reg. Forest	30″, 90″, 300″, 1800″	point	Collelongo	daily/daily	1
Prebas	Reg. Forest	30″, 90″, 300″, 1800″	point	Hyytiälä+Sodankylä	daily/daily	2
TreeMig	Reg. Forest	30″, 90″, 300″, 1800″	spatial	Switzerland	yearly/yearly	10 080
CARAIB	Reg. Forest	30″, 90″, 1800″	spatial	Belgium + Netherlands	2hours / daily	1
ORCHIDEE–MICT	Biomes	30″, 300″, 1800″	point	Tibetan Plateau	30min / daily	137
CWatM	Regional Water	30″, 90″, 300″, 1800″	spatial	Bhima basin	daily/daily	31
GR4J	Regional Water	30″, 90″, 300″, 1800″	spatial	Norway	daily/daily	86
SWAT	Regional Water	30", 90″, 300″, 1800″	spatial	4 basins at Lake Kinneret	daily/monthly	4
SWIM	Regional Water	300″, 1800″	spatial	Zeravshan catchment	daily/daily	1
MITgcm	Lakes	30″, 90″, 300″	spatial	Lake Kinneret	300 s / daily	5
Simstrat	Lakes	30″, 90″, 300″, 1800″	point	32 ISIMIP lakes	300 s / 6hours	32
Labor model	Labor	300″, 1800″	spatial	Global	yearly/yearly	All grid cells

participated (ORCHIDEE), which provided point-scale simulations across the Tibetan Plateau. From the Labor sector, five empirical models provided simulations at two spatial resolutions, spanning a global extent. However, these results were combined and treated as one model result. Because observed labor-force data are not available at the spatial resolution of the climate forcing, direct validation of the high-resolution simulations was not possible. We therefore re-ran the labor model using GHCNd station temperature data and spatially matched the station-based estimates to the labor-force data at the second administrative level. These station-forced simulations served as the reference against which simulations driven by the gridded CHELSA-W5E5 forcing were evaluated.

Tables 1 and 2 provides a summary of the models, their sectors, configurations, and evaluation data. A detailed description of each model setup can be found in Supplementary Material Part A.

2.3. Evaluation framework

2.3.1. Evaluation metrics

To assess both the quality of the climate forcing data (CHELSA-W5E5 v1) and the performance of the impact models, we employed a set of standard evaluation metrics. These include the root mean squared error (RMSE), mean absolute error (MAE) and Kling–Gupta efficiency (KGE).

The RMSE and MAE were normalized by the interquartile range, defined as the difference between the 75th (Q3) and 25th (Q1) percentiles, to reduce sensitivity to outliers compared with normalization using the full range:

$$\mathrm{RMSE} = \sqrt{\frac{1}{n}\sum_{i=1}^{n}(y_i - y_{\mathrm{obs},i})^2} \quad (1)$$

$$\mathrm{NRMSE} = \frac{\mathrm{RMSE}}{Q3 - Q1} \quad (2)$$

$$\mathrm{MAE} = \frac{1}{n}\sum_{i=1}^{n}|y_i - y_{\mathrm{obs},i}| \quad (3)$$

$$\mathrm{NMAE} = \frac{\mathrm{MAE}}{Q3 - Q1}. \quad (4)$$

To capture multiple sources of disagreement beyond magnitude alone, we computed the KGE, which integrates correlation, bias, and variability:

$$\mathrm{KGE} = 1 - \sqrt{(r-1)^2 + (\beta-1)^2 + (\gamma-1)^2} \quad (5)$$

Table 2. Model overview (Part 2 of 2): forcing inputs and evaluation setup.

Impact model	Forcing variables (CHELSA-W5E5)	Add. Forcing variables	Evaluation variables	Evaluation temporal Resolution	Forcing Eval. Benchmark
BBGCMuSo	tasmax, tasmin, pr rsds	day tas, day vpd	GPP, AET	monthly	Local climate data
3D-CMCC-FEM	tas, tasmax, tasmin pr, rsds	rh	GPP, AET	monthly	Local climate data
i3PGmiX	tas, tasmax, tasmin pr, rsds	—	GPP, AET	monthly	Local climate data
4C	tas, tasmax, tasmin pr, rsds	ps, rh	GPP, AET	monthly	Local climate data
3PG-Hydro	tas, tasmax, tasmin pr, rsds	—	GPP, AET	monthly	Local climate data
Prebas	tas, pr, rsds	rh	GPP, AET	monthly	Local climate data
TreeMig	tas, pr	—	basal area	yearly	GHCN-D stations in ±0.125° of eval.locations
CARAIB	tas, tasmax, tasmin pr, rsds	rh, wind	GPP, AET	daily	Local climate data
ORCHIDEE–MICT	tas, tasmax, tasmin pr, rsds	qair, rlds, wind, ps	ALT, MAGT, soil temp.	daily	GHCN-D stations in ±0.125° of eval.locations
CWatM	tas, tasmax, tasmin pr, rsds	rlds, wind, rh, ps	river discharge, res. level	daily	GHCN-D stations in ±0.125° of eval.locations
GR4J	tas, pr	—	river discharge	daily	GHCN-D stations in catchment of eval. location
SWAT	tasmax, tasmin, pr rsds	rh, wind	river discharge	monthly	GHCN-D stations in ±0.125° of eval.locations
SWIM	tas, tasmax, tasmin pr, rsds	—	river discharge	daily	GHCN-D stations in ±0.125° of eval.locations
MITgcm	tas, rsds, pr	rlds, wind, rh, hurs	lake temp. profile	daily	Local climate data
Simstrat	tas, rsds, pr	rlds, wind, ps, hurs	lake temp. profile	6hours	GHCN-D stations in ±0.125° of eval.locations
Labor model	tasmin	rh	diff. to station forc.	yearly	N/A

where:

r = Pearson correlation coefficient between y_i and $y_{\mathrm{obs},i}$

$$\beta = \frac{\mu_y}{\mu_{\mathrm{obs}}} \quad \text{(bias ratio)}$$

$$\gamma = \frac{CV_y}{CV_{\mathrm{obs}}} = \frac{\sigma_y/\mu_y}{\sigma_{\mathrm{obs}}/\mu_{\mathrm{obs}}} \quad \text{(variability ratio)}.$$

KGE values range from $-\infty$ to 1, with 1 indicating a perfect match between model and observation.

Some models were evaluated based on more than one variable (e.g., forest models using both GPP and AET). In those cases, each metric was first computed separately for each variable and then averaged across variables, yielding one RMSE, one MAE, and one KGE value per model, as shown in figure 3.

2.3.2. Evaluation of CHELSA-W5E5 forcing data (30″, 90″, 300″, 1800″)

To evaluate the accuracy of the CHELSA-W5E5 climate forcing dataset at different spatial resolutions (30″, 90″, 300″, and 1800″), we compared the CHELSA-W5E5 climate variables against observations from the global historical climatology network daily (GHCN-D) dataset (Menne *et al* 2018). GHCN-D provides daily meteorological measurements, including 2 m air temperature and precipitation, based on *in situ* weather station data, available for the same period as CHELSA-W5E5 (1979–2016).

For each evaluation site, we used local station climate data wherever possible to evaluate CHELSA-W5E5 forcing data. For the remaining models, we used GHCN-D station data for evaluation. Where catchment boundaries were available, we selected all GHCN-D stations within the catchment; otherwise, we selected stations within ±0.125° of each evaluation location. From the CHELSA-W5E5 dataset, we extracted the grid cell value corresponding to the location of each local/GHCN-D station for all four spatial resolutions. Refer to table 2 to see for which models which approach was applied.

The extracted temperature and precipitation values were then evaluated using the metrics described in section 2.3.1. For each resolution and evaluation location, we computed the mean of each evaluation metric across all available GHCN-D stations within the grid cell. This yielded a single summary value per metric, per resolution, per evaluation site, representing the accuracy of the climate forcing data at that location.

2.4. Terrain descriptors

To quantify topographic complexity, we used the terrain ruggedness index (TRI) as described by Amatulli *et al* (2018). The TRI dataset provides near-global coverage (excluding polar regions) and is derived from the 250 m Global Multi-resolution Terrain Elevation Data 2010 (GMTED2010) dataset (Danielson and Gesch 2011).

TRI is calculated as the mean of the absolute differences in elevation between a center grid cell and its eight surrounding cells. This metric captures the total elevation change within a given neighbourhood: flat terrain results in TRI values close to zero, while steep or mountainous regions yield higher values.

For each model evaluation location, TRI was averaged over a 0.25° grid cell centered on the evaluation point (i.e., ±0.125° in both latitude and longitude).

3. Results

3.1. Evaluation of CHELSA W5E5 across resolutions

We assessed the accuracy of the CHELSA-W5E5 v1 climate forcing dataset across four spatial resolutions by benchmarking it against station observations from the GHCN-D dataset (Menne *et al* 2018). As a representative case, figure 2 illustrates model performance over the European Alps, a region characterized by pronounced topographic heterogeneity. For near-surface temperature, increasing spatial resolution leads to a systematic and spatially coherent reduction in model error, particularly in mountainous terrain. This highlights the substantial value of high-resolution climate forcing in capturing local temperature variability. In contrast, improvements in precipitation are more nuanced. While RMSE values tend to decline slightly from the coarsest (1800″) to the finest (30″) resolution, mean KGE scores increase marginally, and the gains are neither consistent across sites nor uniformly positive.

3.2. Impact model performance across resolutions

When analyzing model performance across all sectors, variables, and locations, we find that increasing the spatial resolution of climate forcing generally improves the accuracy of the impact model (figure 3). The most substantial improvements are observed in models from the forest and biome sectors, reflecting their increased sensitivity to temperature variability and their application in regions of greater topographic complexity (figure 3(c)). In contrast, models in the lakes and water sectors show more modest gains, likely due to their modelling domains in regions of smaller topographic complexity. Water-sector models also rely more heavily on precipitation input, whose accuracy shows less consistent improvement with increasing resolution (as noted in figure 2).

Among all models evaluated, the spatially explicit forest dynamics model TreeMig demonstrates the greatest reduction in normalized RMSE (NRMSE) with finer resolution, underlining the value of high-resolution climate inputs in complex terrain and suggesting that landscape-scale simulations can better exploit high-resolution information than point-scale models. In contrast, the socioeconomic labor model shows reduced performance at intermediate (300″) resolution compared to the coarsest (1800″). This decline is primarily attributable to limitations in the available evaluation data. Because observed labor-force outcomes are not available at the spatial resolution of the climate forcing, the labor simulations were evaluated against reference simulations driven by GHCN-D station temperature data spatially matched to the labor-force dataset at the second administrative level.

Lastly, panel (c) in figure 3 indicates a relationship between terrain complexity and model improvement, suggesting that regions with more pronounced topographic variation benefit the most from increased spatial resolution in climate forcing data.

Illustrative example: resolution effects in a forest dynamics model

To illustrate how these resolution effects manifest at the model and species level, we focus on the forest model *TreeMig*, which simulates basal area per tree species (evaluated against plot-level observations from the Swiss National Forest Inventory, LFI; see Supplementary Material A and B). A spatial comparison for one predominant species (*Larix decidua*) is shown in figure 4, illustrating substantial differences in model output across spatial resolutions. This example highlights that results aggregated across multiple locations and/or variables may obscure resolution-dependent differences that are more evident at finer spatial or species-specific scales.

3.3. Impact model performance vs climate accuracy

We examined how the impact model performance changes with increasing spatial resolution of climate forcing, progressing from 60 km (1800″) to 10 km (300″), then to 3 km (90″), and finally to 1 km (30″). These shifts in model accuracy were evaluated alongside corresponding changes in the accuracy of the underlying climate data (figure 5). For each step, we

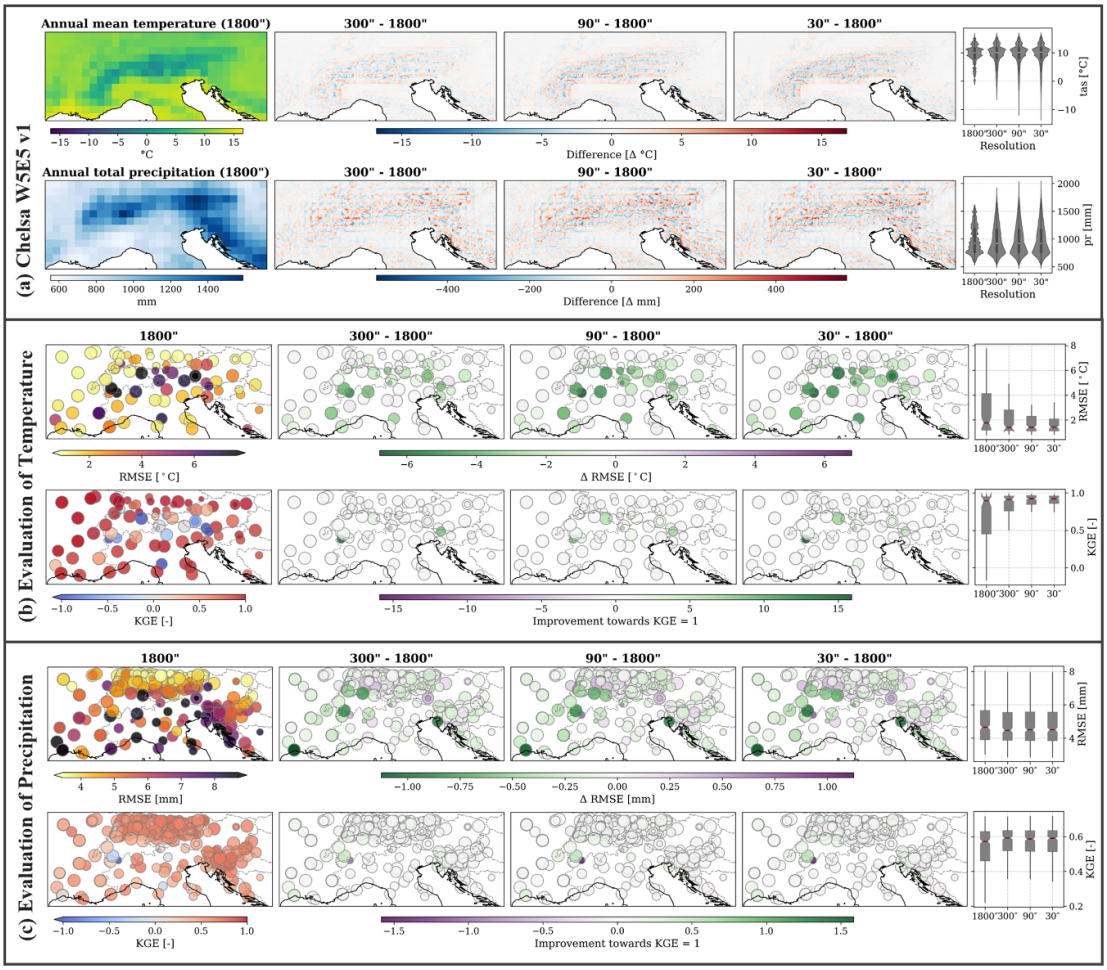


Figure 2. Evaluation of CHELSA-W5E5 v1 climate forcing data at multiple spatial resolutions over the European Alps. Panel (a) shows CHELSA-W5E5 v1 temperature and precipitation at four spatial resolutions. The first column displays absolute values at 1800″ resolution; subsequent columns show differences relative to the 1800″ baseline. Mountainous regions, such as the European Alps, are apparent in the first column of (a) as areas with lower temperatures (bluer shading) and higher precipitation (darker blue shading). Panels (b) and (c) show evaluation against GHCN-D station observations, with dot size indicating the number of daily measurements available per station. The first column presents absolute error metrics for 1800″ resolution; the remaining columns show relative changes in error compared to this baseline. Panel (b) corresponds to temperature, and panel (c) to precipitation. For KGE in the relative-change panels of (b) and (c), the color scale shows changes in the absolute KGE value (i.e. movement toward or away from the ideal value of 1).

computed the percentage change in NRMSE across all impact models with available local climate station data or GHCN-D observations within the hydrologic catchment (where a catchment/watershed outline was available), or within a ±0.125° grid around each evaluation site (see tables 1 and 2 for what was available per model). Temperature and precipitation were assessed separately, as shown in panels (figures 5(a) and (b)), respectively.

For temperature, the largest improvements in both climate input accuracy and model performance occurred in the transition from 60 km to 10 km resolution. Beyond this, gains from increasing resolution further to 3 km and 1 km were more modest. Most evaluation points clustered in the lower-left quadrant of the plots, indicating that improved climate accuracy was generally accompanied by improved model performance.

For precipitation, a similar pattern emerged, although changes in climate accuracy between resolutions were smaller than for temperature, consistent with the evaluation of CHELSA-W5E5 v1 (figure 2). The 60 km–10 km transition yielded the most consistent improvements, again with most points located in the lower-left quadrant. However, in the transition from 10 km to 3 km, some points, particularly for the water sector (GR4J model; see figure S61 in the Supplementary Material Part C for the same plot by model rather than by sector) fell in the upper quadrants, suggesting reduced model performance despite stable climate accuracy. Intriguingly, these same locations showed marked improvement when moving from 3 km to 1 km, even though climate accuracy remained nearly unchanged. These sites lacked co-located temperature observations, pointing to temperature as a likely explanatory variable

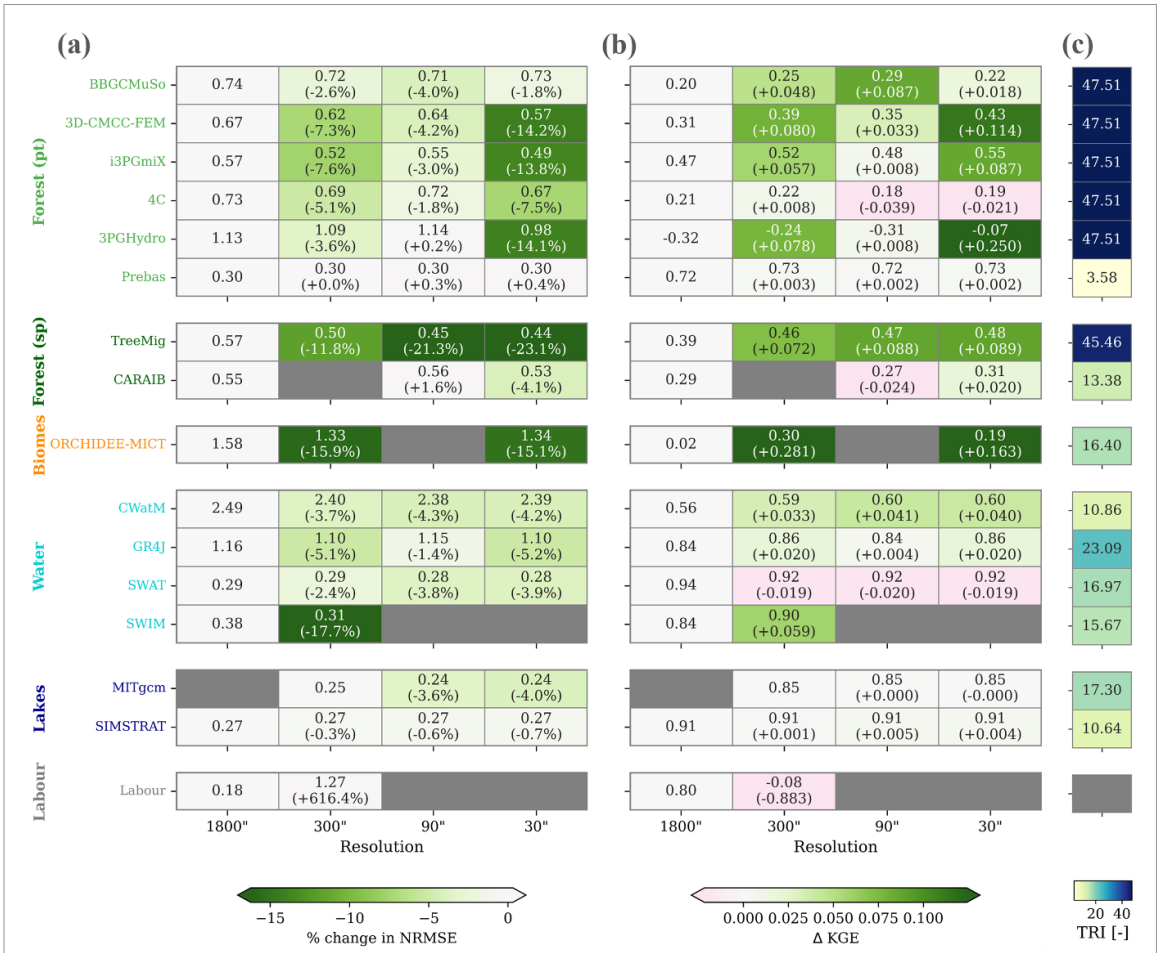


Figure 3. Comparison of NRMSE (interquartile range-normalized) and KGE across spatial resolutions for all participating ISIMIP sectors and models using sector-specific variables and sector-specific temporal scales (daily, monthly, or annual) for the evaluation (see table 2). (a) NRMSE and (b) KGE results from impact model simulations, each evaluated against sector-specific reference data using sector-specific variables. For NRMSE, cell colors indicate the percentage difference in error relative to the coarse 1800″ (∼60 km) resolution (green indicates improvement), while absolute error values are displayed within each cell. For KGE, cell colors indicate the change in KGE relative to the coarse 1800″ resolution, with negative values indicating worse performance and positive values indicating improved performance. Colorbar limits are clipped to the 95th percentile; triangular shaped colorbar indicates values exceeding the scale. Panel (c) shows the mean topographic complexity at each model's evaluation locations. We show the terrain ruggedness index (TRI), which quantifies surface heterogeneity, with higher values (blue on colormap) indicating more complex terrain around the evaluation sites. As the labor sector model was evaluated globally, no TRI was computed.

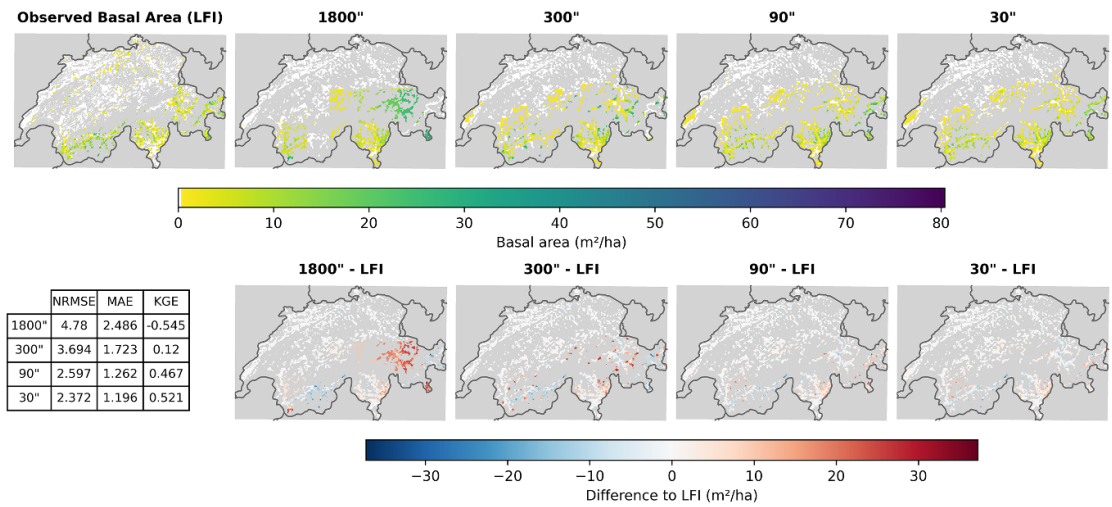
and underscoring the importance of jointly evaluating multiple climate inputs when interpreting spatial resolution effects in impact modeling.

Figure S62 in the Supplementary Material Part C presents the same analysis as figure 5, showing a direct comparison between 1800″ (60 km) and 30″ (1 km) resolution, confirming the trend of improvements in model performance aligning with better climate data.

4. Discussion

We systematically evaluated how changes in the spatial resolution of climate input data affect the predictive performance of a suite of climate impact models participating in ISIMIP. A portfolio of 16 impact models was run using the same global CHELSA-W5E5 v1 climate forcing dataset, varying in spatial resolution from 1800″ to 30″.

Our study demonstrates that increasing the spatial resolution of climate forcing data can improve the accuracy of climate impact models across a range of sectors. These improvements are particularly evident in regions with high topographic complexity, confirming long-standing concerns about the scale mismatch between climate inputs and ecological or socio-environmental processes (Thuiller 2003, Seo *et al* 2009, Hickler *et al* 2012). While prior studies have identified resolution effects in isolated models or sectors (Mearns *et al* 2001, Randin *et al* 2009, Hattermann *et al* 2017, Kumar *et al* 2022), our cross-sectoral experimental setup provides a unique dataset to assess these effects systematically under harmonized conditions. The consistency of the improvements observed—especially for temperature-dependent variables—underscores the value of high-resolution forcing data in impact modeling.



	NRMSE	MAE	KGE
1800"	4.78	2.486	-0.545
300"	3.694	1.723	0.12
90"	2.597	1.262	0.467
30"	2.372	1.196	0.521

Figure 4. Example of spatial results for the tree species Larix decidua simulated with the TreeMig model from the forest sector. Simulated basal area from TreeMig is compared to observational data from the national forest inventory (LFI) across the four spatial resolutions (1800″, 300″, 90″, and 30″). Results show spatial variation, with notable improvements in simulation accuracy at higher resolutions (see NRMSE, MAE and KGE metrics in the lower left corner) - particularly in the eastern mountainous regions. White in the first row indicates species absence; in the second row white indicates no difference between simulated and observed basal area. Grey in both rows indicates missing LFI data.

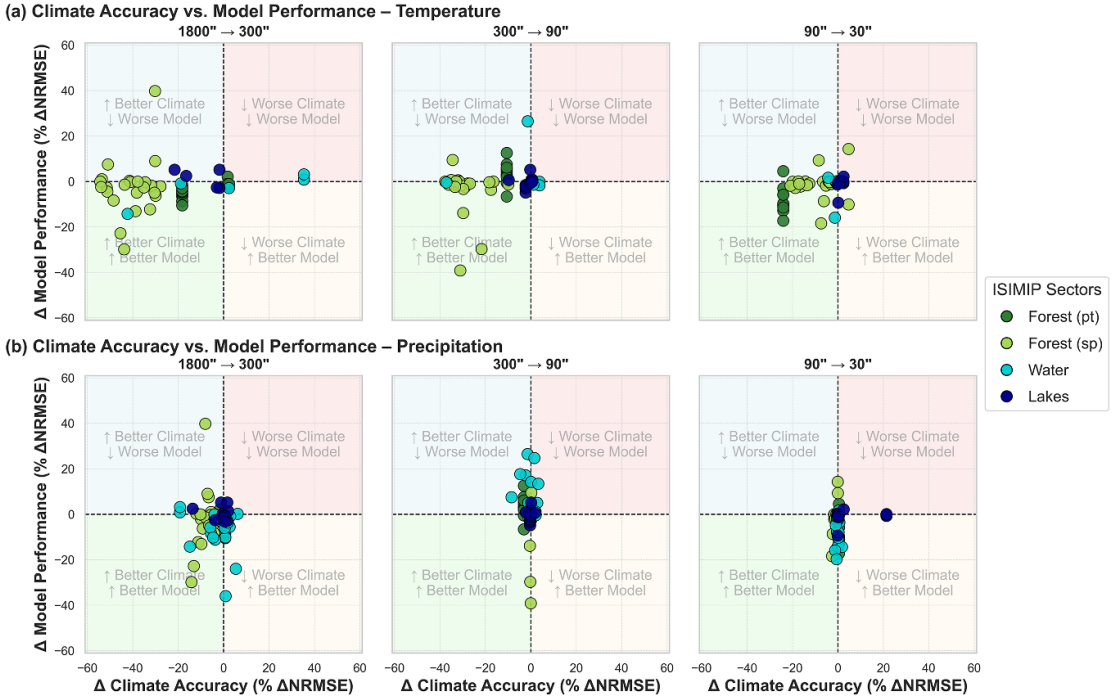


Figure 5. Per-sector comparison of percentage changes in NRMSE for model performance and climate accuracy across spatial resolutions at all model evaluation locations where climate accuracy reference data is available. Panel (a) uses GHCNd temperature station data, and panel (b) uses GHCNd precipitation station data for climate accuracy assessment. In both panels, the subplots from left to right correspond to resolution changes from 1800″ (approximately 60 km) to 300″ (approximately 10 km), from 300″ to 90″ (approximately 3 km), and from 90″ to 30″ (approximately 1 km). Each data point represents a model-variable evaluation pair with co-located GHCNd or local station data. For spatial models, one point is shown per location with a co-located GHCNd station, which is why there can be multiple points for the same model-variable combination. The plots are divided into four quadrants: the green lower-left quadrant represents simultaneous improvement in both climate accuracy and model performance; the blue upper-left quadrant indicates improved climate accuracy but degraded model performance; the yellow lower-right quadrant indicates worse climate accuracy but better model performance; and the red upper-right quadrant indicates a decline in both climate accuracy and model performance.

When disaggregated by sector, the most substantial resolution-driven improvements are observed in the forest and biome models. These systems, which are often tightly coupled to temperature and elevation gradients, benefited from finer spatial representations of climate, particularly in mountainous regions.

Recent studies in the forest sector have demonstrated that the impact of temperature is greater than the impact of precipitation along the environmental gradient (Merganičová *et al* 2024). Models such as *TreeMig*, which are spatially explicit and incorporate heterogeneity over the cells in forest composition and structure, showed notable gains in performance as resolution increased. For the point-scale forest models, an additional scale mismatch should be considered: the observational data represent local tower-footprint conditions, whereas the climate forcing represents an areal mean over the corresponding grid cell. Consequently, changes in model-observation agreement across forcing resolutions may partly reflect changes in spatial representativeness rather than the response of the impact model alone. Conversely, models in the lakes and regional water sectors exhibited more modest benefits, with some even showing reduced performance at intermediate resolutions. For the water sector, this is likely due to their stronger dependence on precipitation forcing, which showed only limited accuracy improvements with increasing resolution, consistent with previous findings on the challenges of precipitation interpolation and downscaling (Daly *et al* 1997, Karger *et al* 2020a). Besides air temperature, lake's sensitivity to spatial resolution is expected to depend primarily on wind speed and radiative fluxes rather than precipitation, because wind controls vertical mixing, entrainment and stratification stability, while shortwave radiation governs the primary heat input to the lake. Precipitation is represented differently by the two lake models and is not expected to be a dominant control on their thermal response. In Simstrat, precipitation is used only to calculate snow accumulation on ice-covered lakes and does not contribute a direct heat or water flux, whereas MITgcm explicitly represents surface freshwater fluxes associated with precipitation and evaporation, alongside the surface heat fluxes. Even in MITgcm, however, the direct thermal effect of precipitation is small compared with radiative, sensible and latent heat fluxes and wind-driven mixing. Consequently, changes in wind and radiation forcing may exert a stronger influence on simulated lake temperatures and stratification dynamics than changes in precipitation. In our analysis, however, climate-forcing evaluation was limited to temperature and precipitation. Although wind and radiation observations are available for Lake Kinneret, these variables were not evaluated systematically across the lake simulations. We therefore cannot determine whether higher-resolution wind and radiation forcing better represents local conditions, limiting our ability to attribute the relatively small changes in lake-model performance specifically to the quality of the meteorological forcing or to the models' response to increased forcing resolution. More generally, several participating models also depend on radiation, humidity, wind, and atmospheric pressure (table 2), so the analysis in figure 5 relates impact-model performance only to the subset of climate drivers that could be independently evaluated. Resolution-dependent changes in model performance therefore cannot always be attributed uniquely to changes in temperature or precipitation accuracy. Furthermore, several participating models, including both lake models, internally operate at sub-daily time steps (300 s for MITgcm and Simstrat), whereas the CHELSA-W5E5 meteorological forcing is provided at daily resolution. This temporal mismatch removes sub-daily forcing variability independent of spatial resolution, potentially masking benefits of finer spatial forcing and making temporal-scale error difficult to separate from spatial-resolution effects. In addition, the lakes and water sector simulations were conducted mainly in regions with relatively low topographic complexity, further limiting the potential benefits of finer spatial resolution.

The empirical labor model presents a distinct case because its evaluation relies on station-forced model simulations rather than direct observations of labor outcomes at the climate-forcing grid scale. The poorer agreement of the 300″ simulations relative to the 1800″ simulations should therefore be interpreted as reduced agreement with this station-forced benchmark, rather than as direct evidence that coarser climate forcing produces more accurate labor impacts. More generally, this highlights the difficulty of evaluating high-resolution socioeconomic impact simulations when observational data are available only at coarser administrative scales. For the labor force, the advantage of using high-resolution data is that it enables the identification of locations where workers are particularly vulnerable due to a combination of increasing heat, workplace setting (including indoor or outdoor work), and person-specific attributes, thereby helping to identify where context-specific labor protection policies are likely to have the greatest impact on health and economic outcomes.

From a methodological perspective, our results support the increasing emphasis in climate impact research on harmonized input data and protocol standardization, as exemplified by initiatives such as ISIMIP (Frieler *et al* 2017, 2024). While previous ensemble modeling efforts have primarily focused on capturing structural and parametric uncertainty (Knutti and Sedláček 2013, Eyring *et al* 2016, Collalti *et al* 2019), our findings show that spatial resolution is an equally critical factor, particularly when high-resolution data are applied consistently across sectors.

While the advantages of high-resolution climate data are evident in many contexts, our

results also highlight several important limitations. An important limitation of the experimental design is that the four forcing resolutions are not independently-generated climate products: the 90″, 300″, and 1800″ fields are spatial aggregations of the same underlying 30″ CHELSA-W5E5 fields. Our experiment therefore primarily isolates sensitivity to the progressive removal of fine-scale spatial information from a common underlying forcing dataset, rather than differences among independently generated climate products at different nominal resolutions. This design reduces confounding effects from product-specific biases and methodological differences, but spatial aggregation also smooths small-scale variability and extremes. Consequently, the differences observed between resolutions may be smaller than those obtained when comparing independently generated climate products. A further limitation concerns the geographic coverage of the evaluation. The quantitative magnitude of the resolution effects reported here should not be extrapolated uniformly to all regions. With the exception of the globally evaluated labor model, evaluation locations are concentrated in Europe, with additional sites on the Tibetan Plateau and in selected catchments and lakes elsewhere, while tropical and arid systems remain comparatively underrepresented. In addition, the computational and storage demands of running impact models at high spatial resolution are substantial, especially for gridded models operating over large spatial domains. This limits practical applicability, particularly for global-scale simulations or long-term projections. Moreover, finer resolution does not automatically guarantee better model performance. In several cases—especially for precipitation—higher resolution introduced noise or errors, likely due to uncertainties in the downscaling process or mismatches with the spatial scale of observational validation data. These mixed results underscore the importance of local context and caution against assuming uniform benefits of high-resolution precipitation input when evaluating downstream model performance. These findings are consistent with concerns in the literature about the challenges of accurately representing small-scale precipitation variability using interpolation-based methods (Daly *et al* 1997, Karger *et al* 2017, 2020a). Targeted efforts to improve both the density and quality of precipitation observations, as well as the associated downscaling methods, are therefore crucial. Moreover, for some impact models, finer-scale climate inputs can fall below the spatial or temporal scales for which model structures and parameters were designed, causing models calibrated at coarser resolutions to respond weakly or artefactually to added small-scale variability (Maraun 2016, Maurer *et al* 2016). For the lake models, different calibration strategies were used across forcing resolutions. Simstrat was recalibrated at each resolution, consistent with its standard workflow and to avoid favoring the resolution used for calibration, whereas MITgcm retained the same parameter set across resolutions to isolate the direct response to forcing resolution. These differing approaches should be considered when comparing resolution sensitivity between the two models. This highlights that increasing input resolution alone may be insufficient and motivates efforts to improve both model process representation and downscaling and bias-correction methods so that high-resolution climate forcings can be used effectively. Lastly, as demonstrated by the labor-sector model, the benefits of higher-resolution input data are more difficult to evaluate when observational datasets are unavailable at comparable spatial resolution. Without appropriate validation data, the magnitude of these benefits may remain uncertain.

Acknowledgments

This article benefited from COST Action CA19139 PROCLIAS (PROcess-based models for CLimate Impact Attribution across Sectors), as well as COST Action CA24163 CROSS-CASCADE (Modelling cross-sectoral cascading climate impacts on Europe to design coherent policy responses), both supported by COST (European Cooperation in Science and Technology; www.cost.eu, last access: 15 October 2025). Johanna Malle and Dirk Nikolaus Karger received funding from the funding organization of the Swiss National Science Foundation (SNF; project Adohris, 205530). Xue Yang would like to acknowledge grant support from the National Natural Science Foundation of China (Grant No. 52209035). Elad Ben-Zur was supported by a grant from the Israeli Ministry of Science and Technology (#4755). Iulii Didovets and Fred F. Hattermann would like to acknowledge funding from the Green Central Asia initiative—Enhancing environment, climate and water resilience. Laura Dobor was supported by the Czech Science Foundation (GAČR), grant number 26-20790N. Merganičová, Katarína was funded by the EU NextGenerationEU through the Recovery and Resilience Plan for Slovakia under the project No. 09I03-03-V04-00130. Observational data for the TreeMig model was made available by the Schweizerisches Landesforstinventar LFI (Daten der Erhebung 1983–85 (LFI1), Esther Thürig-DL1619. Eidg. Forschungsanstalt WSL, Birmensdorf). We thank Katja Frieler, Matthias Mengel, Jacob Schewe and Stefan Lange for insightful discussions during this project, and Lisa Novak for her assistance with data harmonisation.

Data availability statement

The data that support the findings of this study are openly available at the following URL/DOI: https://doi.org/10.5281/zenodo.17940720 and https://doi.org/10.48364/ISIMIP.437390.

Supplementary Information available at https://doi.org/10.1088/1748-9326/aeb279/data1.

Author contributions

J.T.M., C.P.O.R., and D.N.K. conceived the study, developed the methodology, and coordinated the simulations. J.T.M. performed the analysis with input from C.P.O.R. and D.N.K. J.T.M. wrote the original draft, and D.N.K. supervised the project and acquired funding. Y.A., A.L.D.A., Y.B.-S., E.B.-Z., P.B., T.C., J.C., A.C., D.D., S.D., I.D., M.D., L.D., L.F., S.N.G., F.H., S.H., H.L., T.L., K.M., F.M., M.N., E.J.Z.R., M.S., M.S., R.S., E.V., X.Y., and R.Y. provided simulation results and observational data used in this study and are listed in alphabetical order. A.I.A. and D.M.-B. coordinated the sectoral modelling efforts and are listed in alphabetical order. D.Q.-C. supported ISIMIP's provision and development of climate data. All authors contributed to manuscript review and editing.

Data and code availability

The CHELSA-W5E5 v1.0 climate data used in this study are available from the ISIMIP repository at https://data.isimip.org/search/query/CHELSA-W5E5%20v1.0/, hosted and maintained by the Potsdam Institute for Climate Impact Research (PIK). The code used to evaluate the climate data and model results and to generate all figures is available on GitHub at https://github.com/johanna-malle/isimip-highres-sensitivity-experiments. The datasets required to run the code, including the processed simulation outputs and input data used to reproduce the figures, are available on Zenodo at https://doi.org/10.5281/zenodo.17940720. All raw simulation outputs are available through the ISIMIP data repository at https://doi.org/10.48364/ISIMIP.437390.

ORCID iDs

Johanna T Malle 0000-0002-6185-6449
Christopher P O Reyer 0000-0003-1067-1492
Yael Amitai 0000-0002-6113-7727
Andrey L D Augustynczik 0000-0001-5513-5496
Peter Burek 0000-0001-6390-8487
Tarunsinh Chaudhari 0009-0000-7818-2869
Jinfeng Chang 0000-0003-4463-7778
Alessio Collalti 0000-0002-4980-8487
Daniela Dalmonech 0000-0002-1932-5011
Shouro Dasgupta 0000-0003-4080-8066
Iulii Didovets 0000-0003-1169-6165
Marc Djahangard 0000-0001-9550-6343
Laura Dobor 0000-0001-6712-9827
Simon N Gosling 0000-0001-5973-6862
Fred F Hattermann 0000-0002-6046-4670
Shaochun Huang 0000-0001-7426-5181
Heike Lischke 0000-0003-4284-5194
Francesco Minunno 0000-0002-7658-6402
Mats Nieberg 0000-0002-9755-8814
Elizabeth J Z Robinson 0000-0002-4950-0183
Martin Schmid 0000-0001-8699-5691
Mikhail Smilovic 0000-0001-9651-8821
Ritika Srinet 0000-0002-2957-7626
Elia Vangi 0000-0002-9772-2258
Daniel Mercado-Bettin 0000-0003-4572-3029
Dánnell Quesada-Chacón 0000-0001-5700-1846
Dirk N Karger 0000-0001-7770-6229

References

Aerts J P M, Hut R W, Giesen N C, Drost N, Verseveld W J, Weerts A H and Hazenberg P 2022 Large-sample assessment of varying spatial resolution on the streamflow estimates of the wflow_sbm hydrological model *Hydrol. Earth Syst. Sci.* **26** 4407–30

Amatulli G, Domisch S, Tuanmu M-N, Parmentier B, Ranipeta A, Malczyk J and Jetz W 2018 A suite of global, cross-scale topographic variables for environmental and biodiversity modeling *Sci. Data* **5** 180040

Baño-Medina J, Manzanas R, Cimadevilla E, Fernández J, González-Abad J, Cofiño A S and Gutiérrez J M 2022 Downscaling multi-model climate projection ensembles with deep learning (deepesd): contribution to cordex eur-44 *Geosci. Model Dev.* **15** 6747–58

Barnhart T B, Putman A L, Heldmyer A J, Rey D M, Hammond J C, Driscoll J M and Sexstone G A 2024 Evaluating distributed snow model resolution and meteorology parameterizations against streamflow observations: finer is not always better *Water Resour. Res.* **60** e2023WR035982

Berndt C, Diedrich H, Früh B, Hofmann M, Kruschke T, Leuprecht A and Zimmer J 2018 Climate services for germany: first experiences of national provision of climate information *Clim. Serv.* **9** 1–9

Bottazzi M *et al* 2024 High performance computing to support land, climate and user-oriented services: the highlander data portal *Meteorol. Appl.* **31** e2166

Briggs W M and Cogley J G 1996 Topographic bias in climatological observations of precipitation due to coarseness of the grid *J. Geophys. Res.: Atmos.* **101** 2611–9

Caminade C, Kovats S, Rocklov J, Tompkins A M, Morse A P, Colón-González F J, Stenlund H, Martens P and Lloyd S J 2014 Impact of climate change on global malaria distribution *Proc. Natl Acad. Sci.* **111** 3286–91

Chen D *et al* 2021 Climate Change 2021: the physical science basis *Contribution of Working Group I to the Sixth Assessment Report of the Intergovernmental Panel on Climate Change* (Cambridge University Press) pp 147–286

Ciscar J-C, Rising J, Kopp R E and Feyen L 2019 Assessing future climate change impacts in the eu and the usa: insights and lessons from two continental-scale projects *Environ. Res. Lett.* **14** 084010

Collalti A, Thornton P E, Cescatti A, Rita A, Borghetti M, Nolé A, Trotta C, Ciais P and Matteucci G 2019 The sensitivity of the forest carbon budget shifts across processes along with stand development and climate change *Ecol. Appl.* **29** e01837

Cramer W et al 2001 Global response of terrestrial ecosystem structure and function to co_2 and climate change: results from six dynamic global vegetation models *Global Change Biol.* **7** 357–73
Cucchi M, Weedon G P, Amici A, Bellouin N, Lange S, Müller Schmied H, Hersbach H and Buontempo C 2020 Wfde5: bias-adjusted ERA5 reanalysis data for impact studies *Earth Syst. Sci. Data* **12** 2097–120
Daly C, Taylor G H, Gibson W P, Parzybok T W, Johnson G H and Pasteris P A 1997 High-quality spatial climate data sets for the united states and beyond *Trans. ASAE* **43** 1957–62
Danielson J J and Gesch D B 2011 Global multi-resolution terrain elevation data 2010 (GMTED2010) *Open-File Report* 2011-1073 U.S. Geological Survey. Earth Resources Observation and Science (EROS) Center
Dasgupta S, Maanen N, Gosling S N, Piontek F, Otto C and Schleussner C-F 2021 Effects of climate change on combined labour productivity and supply: an empirical, multi-model study *Lancet Planet. Health* **5** e455–e465
Dipankar A, Stevens B, Heinze R, Moseley C, Zängl G, Giorgetta M and Brdar S 2015 Large eddy simulation using the general circulation model icon *J. Adv. Model. Earth Syst.* **7** 963–86
Engler R and Guisan A 2009 Migclim: predicting plant distribution and dispersal in a changing climate *Divers. Distrib.* **15** 590–601
Eyring V, Bony S, Meehl G A, Senior C A, Stevens B, Stouffer R J and Taylor K E 2016 Overview of the coupled model intercomparison project phase 6 (CMIP6) experimental design and organization *Geosci. Model Dev.* **9** 1937–58
Frieler K et al 2017 Assessing the impacts of 1.5 °c global warming – simulation protocol of the inter-sectoral impact model intercomparison project (ISIMIP2B) *Geosci. Model Dev.* **10** 4321–45
Frieler K et al 2024 Scenario setup and forcing data for impact model evaluation and impact attribution within the third round of the inter-sectoral impact model intercomparison project (ISIMIP3A) *Geosci. Model Dev.* **17** 1–51
Fuhrer O, Osuna C, Lapillonne X, Gysi T, Cumming B, Bianco M, Arteaga A, Schár C and Wedi N 2018 Near-global climate simulation at 1 km resolution: establishing a performance baseline on 4888 gpus with cosmo 5.0 *Geosci. Model Dev.* **11** 1665–81
Goderniaux P, Brouyère S, Blenkinsop S, Burton A, Fowler H J, Orban P and Dassargues A 2011 Modeling climate change impacts on groundwater resources using transient stochastic climatic scenarios *Water Resour. Res.* **47** W12516
Habibullah M S, Din B H, Tan S-H and Zahid H 2022 Impact of climate change on biodiversity loss: Global evidence *Environ. Sci. Pollut. Res.* **29** 1073–86
Harris N L et al 2021 Global maps of twenty-first century forest carbon fluxes *Nat. Clim. Change* **11** 234–40
Harrison P A, Dunford R W, Holman I P and Rounsevell M D A 2016 Climate change impact modelling needs to include cross-sectoral interactions *Nat. Clim. Change* **6** 885–90
Hattermann F F et al 2017 Cross-scale intercomparison of climate change impacts simulated by regional and global hydrological models in eleven large river basins *Clim. Change* **141** 561–76
Hickler T et al 2012 Projecting the future distribution of european potential natural vegetation zones with a generalized, tree species-based dynamic vegetation model *Glob. Ecol. Biogeogr.* **21** 50–63
Isaac M and van Vuuren D P 2009 Modeling global residential sector energy demand for heating and air conditioning in the context of climate change *Energy Policy* **37** 507–21
Jägermeyr J et al 2021 Climate impacts on global agriculture emerge earlier in new generation of climate and crop models *Nat. Food* **2** 873–85
Jones E R et al 2025 A multi-model assessment of global freshwater temperature and thermoelectric power supply under climate change *Environ. Res.: Water* **1** 025002
Karger D N et al 2020 Climatologies at high resolution for the earth's land surface areas *Sci. Data* **4** 170122
Karger D N, Conrad O, Böhner J, Kawohl T, Kreft H, Soria-Auza R W, Zimmermann N E, Linder H P and Kessler M 2017 Climatologies at high resolution for the earth's land surface areas *Sci. Data* **4** 170122
Karger D N, Lange S, Hari C, Reyer C P O, Conrad O, Zimmermann N E and Frieler K 2023 CHELSA-W5E5: daily 1 km meteorological forcing data for climate impact studies *Earth Syst. Sci. Data* **15** 2445–64
Karger D N, Saladin B, Wüest R O, Graham C H, Zurell D, Mo L and Zimmermann N E 2023 Interannual climate variability improves niche estimates for ectothermic but not endothermic species *Sci. Rep.* **13** 12538
Karger D N, Wilson A M, Mahony C, Zimmermann N E and Jetz W 2021 Global daily 1 km land surface precipitation based on cloud cover-informed downscaling *Sci. Data* **8** 307
Keller A A, Garner K L, Rao N, Knipping E and Thomas J 2022 Downscaling approaches of climate change projections for watershed modeling: review of theoretical and practical considerations *PLOS Water* **1** e0000046
Kidd C, Huffman G, Wilheit T, Ferraro R, Joyce R, Hsu K and Braithwaite D 2017 GPM satellite constellation overview and applications to precipitation monitoring *Remote Sens.* **9** 382
Knutti R and Sedláček J 2013 Robustness and uncertainties in the new CMIP5 climate model projections *Nat. Clim. Change* **3** 369–73
König C, Karger D N, Cord A F, Sauermann J, Kreft H, Zimmermann N E, Thuiller W and Zurell D 2021 Scale dependency of joint species distribution models challenges interpretation of biotic interactions *J. Biogeogr.* **48** 839–50
Kumar A et al 2022 Multi-model evaluation of catchment- and global-scale hydrological model simulations of drought characteristics across eight large river catchments *Adv. Water Resour.* **165** 104212
Lange S 2019 WFDE5 over land merged with ERA5 over the ocean (w5e5) *ISIMIP* (available at: https://doi.org/10.48364/ISIMIP.342217)
Lawrence D, Coe M, Walker W, Verchot L and Vandecar K 2022 The unseen effects of deforestation: biophysical effects on climate *Front. For. Glob. Change* **5** 5
Lee H et al 2023 Climate change 2023: synthesis report. contribution of working groups I, II and III to the sixth assessment report of the intergovernmental panel on climate change *IPCC*
Magnusson J, Eisner S, Huang S, Lussana C, Mazzotti G, Essery R, Saloranta T and Beldring S 2019 Influence of spatial resolution on snow cover dynamic for a coastal and mountainous region at high latitudes (norway) *Water Resour. Res.* **55** 5612–30
Malle J 2025 Figure reproduction data for high-resolution climate input sensitivity in ISIMIP models (version 1.0.0.) *Zenodo* (available at: https://doi.org/10.5281/zenodo.17940720)
Malle J et al 2026 ISIMIP3a high-resolution sensitivity experiment (version 1.0) *ISIMIP Repository* (available at: https://doi.org/10.48364/ISIMIP.437390)
Maraun D 2016 Bias correcting climate change simulations - a critical review *Curr. Clim. Change Rep.* **2** 211–20
Maurer E P, Ficklin D L and Wang W 2016 Technical note: the impact of spatial scale in bias correction of climate model output for hydrologic impact studies *Hydrol. Earth Syst. Sci.* **20** 685–96
McMaster G and Wilhelm W 1997 Growing degree-days: one equation, two interpretations *Agric. For. Meteorol.* **87** 291–300
Mearns L O, Easterling W, Hays C and Marx D 2001 Comparison of agricultural impacts of climate change calculated from high and low resolution climate change scenarios: I. The uncertainty due to spatial scale *Clim. Change* **51** 131–72
Meehl G A, Boer G J, Covey C, Latif M and Stouffer R J 2000 The coupled model intercomparison project (CMIP) *Bull. Am. Meteorol. Soc.* **81** 313–8
Meehl G A, Covey C, Delworth T, Latif M, McAvaney B, Mitchell J F B, Stouffer R J and Taylor K E 2007 The WCRP

CMIP3 multimodel dataset: A new era in climate change research *Bull. Am. Meteorol. Soc.* **88** 1383–94
Menne M J, Bryant J A, Korzeniewski S M, Kristy T, Xungang Y, Anthony S, Ray R, Vose R S, Gleason B E and Houston T G 2018 *Global Historical Climatology Network - Daily (Ghcn-Daily), Version 3.* (*NOAA National Climatic Data Center*)
Merganičová K *et al* 2024 The biogeochemical model Biome-BGCMUSO v6.2 provides plausible and accurate simulations of the carbon cycle in central european beech forests *Geosci. Model Dev.* **17** 7317–46
Neumann P, Düben P, Adamidis P, Bauer P, Brück M, Kornblueh L, Klocke D, Stevens B, Wedi N and Biercamp J 2019 Assessing the scales in numerical weather and climate predictions: will exascale be the rescue? *Phil. Trans. R. Soc. A* **377** 20180148
Pfenning-Butterworth A, Buckley L B, Drake J M, Farner J E, Farrell M J, Gehman A-L M, Mordecai E A, Stephens P R, Gittleman J L and Davies T J 2024 Interconnecting global threats: climate change, biodiversity loss and infectious diseases *Lancet Planet. Health* **8** e270–83
Raffa M, Adinolfi M, Reder A, Marras G F, Mancini M, Scipione G, Santini M and Mercogliano P 2023 Very high resolution projections over italy under different CMIP5 IPCC scenarios *Sci. Data* **10** 238
Randin C F, Engler R, Normand S, Zappa M, Zimmermann N E, Pearman P B, Vittoz P, Thuiller W and Guisan A 2009 Climate change and plant distribution: local models predict high-elevation persistence *Global Change Biol.* **15** 1557–69
Reder A, Fedele G, Manco I and Mercogliano P 2025 Estimating pros and cons of statistical downscaling based on EQM bias adjustment as a complementary method to dynamical downscaling *Sci. Rep.* **15** 621
Reyer C P O, Lasch-Born P, Suckow F, Gutsch M, Murawski A and Pilz T 2014 Projections of regional changes in forest net primary productivity for different tree species in Europe driven by climate change and carbon dioxide *Ann. Forest Sci.* **71** 211–25
Ridder N N, Pitman A J, Westra S, Ukkola A, Do H X, Bador M, Hirsch A L, Evans J P, Di Luca A and Zscheischler J 2020 Global hotspots for the occurrence of compound events *Nat. Commun.* **11** 5956
Schär C *et al* 2019 Kilometer-scale climate models: prospects and challenges *Bull. Am. Meteorol. Soc.* **101** E567–87
Schipper E L F, Dubash N K and Mulugetta Y 2021 Climate change research and the search for solutions: rethinking interdisciplinarity *Clim. Change* **168** 18
Schneider U, Becker A, Finger P, Meyer-Christoffer A, Ziese M and Rudolf B 2014 GPCC's new land surface precipitation climatology based on quality-controlled in situ data and its role in quantifying the global water cycle *Theor. Appl. Climatol.* **115** 15–40
Schulthess T C, Bauer P, Wedi N, Fuhrer O, Hoefler T and Schár C 2018 Reflecting on the goal and baseline for exascale computing: a roadmap based on weather and climate simulations *Comput. Sci. Eng.* **21** 30–41
Seo C, Thorne J H, Hannah L and Thuiller W 2009 Scale effects in species distribution models: implications for conservation planning under climate change *Biol. Lett.* **5** 39–43
Smith M W, Willis T, Mroz E, James W H M, Klaar M J, Gosling S N and Thomas C J 2024 Future malaria environmental suitability in Africa is sensitive to hydrology *Science* **384** 697–703
Sun L and Lan Y 2021 Statistical downscaling of daily temperature and precipitation over china using deep learning neural models: localization and comparison with other methods *Int. J. Climatol.* **41** 1128–47
Tabios G Q and Salas J D 1985 A comparative analysis of techniques for spatial interpolation of precipitation *JAWRA J. Am. Water Resour. Assoc.* **21** 365–80
Thornton P E, Running S W and White M A 1997 Generating surfaces of daily meteorological variables over large regions of complex terrain *J. Hydrol.* **190** 214–51
Thuiller W 2003 Biomod - optimizing predictions of species distributions and projecting potential future shifts under global change *Glob. Change Biol.* **9** 1353–62
Wada Y, Graaf I E M and Beek L P H 2016 High-resolution modeling of human and climate impacts on global water resources *J. Adv. Model. Earth Syst.* **8** 735–63
Wang K, Liu X, Cui P, Zhang Y, Xie J, Liu C and Gosling S N 2025 China's nationwide streamflow decline driven by landscape changes and human interventions *Sci. Adv.* **11** eadu8032
Wood A W, Leung L R, Sridhar V and Lettenmaier D P 2004 Hydrologic implications of dynamical and statistical approaches to downscaling climate model outputs *Clim. Change* **62** 189–216
Woolway R I, Jennings E, Shatwell T, Golub M, Pierson D C and Maberly S C 2021 Lake heatwaves under climate change *Nature* **589** 402–7
Zani D, Lischke H and Lehsten V 2023 Climate and dispersal limitation drive tree species range shifts in post-glacial Europe: results from dynamic simulations *Front. Ecol. Evol.* **11** 1321104
Zapata V, Gernaat D E H J, Yalew S G, Santos da Silva S R, Iyer G, Hejazi M and Vuuren D P 2022 Climate change impacts on the energy system: a model comparison *Environ. Res. Lett.* **17** 034036
Zscheischler J, Westra S, Van Den Hurk B J J M, Seneviratne S I, Ward P J, Pitman A, AghaKouchak A, Bresch D N, Leonard M and Wahl T 2018 Future climate risk from compound events *Nat. Clim. Change* **8** 469–77